Spectroscopies I Have Known—Award Address: Philips ACS Award in Applied Polymer Science

J. L. KOENIG

The Donnell Institute Professor, Department of Macromolecular Science, Case Western Reserve University, Cleveland, Ohio 44106-7202

ABSTRACT: This review paper demonstrates the development of a number of spectroscopic techniques for the characterization of polymers including dispersive infrared, laser-excited Raman spectroscopy, Fourier transform infrared spectroscopy, solid-state nuclear magnetic resonance spectroscopy, and nuclear magnetic resonance imaging. A discussion is given of the roles that these techniques have in the arsenal of the polymer scientist and the nature of the contributions from the author's laboratory. © 1998 John Wiley & Sons, Inc. J Appl Polym Sci 70: 1359–1370, 1998

Key words: spectroscopy; Raman; FTIR; solid-state NMR; NMR imaging; FTIR imaging

INTRODUCTION

The advancements that have occurred over the last 35 years in theory, experimentation, and instrumentation for the characterization of synthetic polymer systems are astonishing when observed from the perspective of the 21st century. The most obvious change is the transition from analog to digital measurements with the development of the computer. It has been my good fortune to have had the opportunity to be a part of these changes in a number of different spectroscopic techniques. In this article, a brief chronological review of some of these developments will be given as well as some observations about the present state of the art and its future developments.

DISPERSION INFRARED SPECTROSCOPY

The grating dispersion spectrometers of the 1960s were quality instruments from a measurement point of view but were limited by their inherent nature to signal-to-noise ratios that were very low by present standards due to the slits required to isolate the dispersed frequencies into resolvable domains. Signal averaging was limited by the difficulty of reproducing the frequencies, and at that time, microcomputers were unavailable so digitization and data processing were limited. We interfaced a main-frame computer, using punched paper tape, to a dispersion spectrometer and used it to make measurements of stereoregularity in polypropylene.[1]

The problems in polymer characterization in the 1960s are not much different from modern-day problems. Polymers are complex multicomponent systems requiring careful band assignments to structural components. Polymer band assignments are made using model compounds, normal coordinates, and correlation with other physical measurements.

Polymer-chain Microstructure

New (at that time) concepts in polymer-chain microstructure such as stereoregularity (initially, the domain of NMR) required both theoretical[2] and experimental analysis[3] to allow the use of

infrared (IR) for this analysis. The selectivity, sensitivity, and speed of the measurement make IR a practical tool for this measurement. The experimental problems concerned proper sample preparation as polymers exhibit high absorbance and must be optically thin for proper measurements.

Positional isomerism in PVF was studied by carrying out optical subtraction of samples polymerized at different temperatures.[4] The results indicated that the positional isomerism, that is the head-to-head and head-to-tail structural contributions, are highly dependent on polymerization temperature.

Chain Folding in Polymers

The use of IR to study morphological components of semicrystalline polymers was initiated for the first time[5] and an entire series of studies of chain folding for a variety of polymers followed. The precise nature of the "elusive" chain fold continues to this day but IR and Raman have made significant contributions to our current state of understanding.[6−18] We finally isolated the illusive "fold band" of polyethylene using FTIR and systematic subtraction.[19,20]

Polymer-chain Orientation

Engineering polymers are generally anisotropic in character and the anisotropy is designed to develop the maximum useful mechanical properties. The properties along a particular directions are affected by the conditions of stretching along that direction. Uniaxial materials, such as fibers, are produced by stretching in one direction, while biaxial materials, such as films, are produced by stretching in two mutually perpendicular directions.

Injection-molded articles of amorphous polymers exhibit an anisotropy in the optical and mechanical properties due to frozen-in orientation of the polymer chains. To a large extent, this orientation is created during the mold-filling stage where the polymer molecules tend to orient while flowing under the action of the prevailing stress field. If the molten polymer is cooled rapidly to a temperature below its glass transition, the polymer molecules will not have sufficient time to relax their orientation and return to a random configuration. There is also a distribution of orientation in the injected-molded article, since polymer molecules at different locations of the final molded part have generally experienced different thermal conditions due to the thermal gradients in the molds.

A high degree of alignment is the basis of improved mechanical, optical, and electrical properties in almost all polymers. Consequently, it is necessary to understand the correlations among molecular order, material properties, and fabrication procedures. Experimental characterization of the degree and direction of alignment is required in order to understand how molecular design and processing strategies lead to the ultimate state of alignment. In polymer structures, orientation will not be complete and distributions of directions of planes or axes will be observed.

For an oriented solid sample, in order for the IR light to be absorbed, a component of the oscillating electric-field vector of the incident light must be oriented in a plane parallel to the electric dipole transition moment. Light polarized perpendicular to the dipole transition moment will not be absorbed.

When the absorbing groups are oriented as in solids, they exhibit IR absorptions that depend not only on how many groups are present in the sample but also on how the groups are oriented with respect to the beam. By using linearly polarized IR radiation, the orientation of the functional groups in a polymer system can be measured.

Measurement of IR linear dichroism requires light polarized both parallel and perpendicular to a fixed reference direction of the sample. For parallel polarized light, the absorbance is termed $A_{\parallel}$, and the absorbance with perpendicular polarized light is termed $A_{\perp}$. The dichroic ratio, R, is defined as

$$R = A_{\parallel}/A_{\perp}$$

For random orientation, $R = 1$. The measured absorption bands are generally classified as parallel (π bands) or as perpendicular (σ bands) depending on whether R is greater or less than 1. This classification of the dichroic behavior is helpful in assigning the various modes to the symmetry types of the normal modes in polymers.[21] The character table of the symmetry group lists the symmetry species of translational motions along the x, y, and z axes as well as the symmetry species of the six components of polarizability. The IR-active vibrations have their transition moments preferentially parallel to the corresponding x, y, and z axes depending on the symmetry type. If z is the fixed reference direction, the IR bands can be classified parallel or perpendicular based

on whether R is greater or less than 1. This dichroic information is useful for structural analysis of polymers as well as in determining the relative orientation of polymer chains in an oriented system.

For unidirectional molecular orientations, such as for uniaxially drawn polymers, the dichroic ratio can be related to the Herman orientation function, F. This quantity is equivalent to the second moment of the orientation distribution function for the molecular axis and is given by

$$f = \langle 3 \cos^2 \theta - 1 \rangle / 2$$

The orientation angle θ is the angle between the draw direction and the local molecular chain axis. The Herman function is equal to 1 when the chain axis is parallel to the film orientation, 0 when the system is randomly oriented, and $\frac{1}{2}$ when the chain axis is perpendicular to the film-orientation direction. This function can be calculated from measurements of the dichroic ratio by using

$$f = [(R - 1)(R_0 + 2)]/[(R + 2)/(R_0 - 1)]$$

where R_0 is the dichroic ratio for perfect uniaxial order. The value of the constant R_0 is unknown and can be different for every IR band studied. For perfect uniaxial order, it is assumed that the polymer chains are all oriented parallel to the draw direction, and the transition moments associated with the vibrations lie on a cone with a semiangle ψ to the chain axis direction. The dichroic ratio is then expressed by

$$\mathbf{R_0 = [2 \cot^2 \psi]}$$

As ψ varies from 0 to π, R_0 varies from 0 to infinity. No dichroism ($R_0 = 1$) will be observed for $\psi = 54°44'$ (the *magic angle*). If the direction of the transition moment with respect to the chain axis is known, the average orientation of the chain segments can be determined from the measured dichroic ratio.

Fortunately, the Herman orientation function, f, can be determined by a number of independent techniques, including X-ray diffraction, birefringence, sonic modulus, and refractive index measurements. These methods, coupled with IR dichroic measurements of absorption, can be used to calculate quantitative values for the transition-moment angles. A plot of f measured by X-ray diffraction versus $(R - 1)/(R + 2)$ will be linear with a zero intercept. A least-squares evaluation of the data from this line will yield the slope, $(R_0 + 2)/(R_0 - 1)$. When ψ is 0° (parallel to the molecular chain axis), the slope equals 1.0 and when ψ_n equals 90°, the slope equals -2.0.

The major advantage of IR (and Raman) for making polarization measurements relative to the X-ray method is that the orientation of the amorphous phase can be determined.[22] A number of different polymers systems have been studied by IR dichroic measurements and a trichroic method has been described which measures the orientation in all three mutually perpendicular directions.[23] In more recent times, the trichroic method has been applied with success to studies of orientation in PET[24,25] and PVF$_2$.[26]

LASER-EXCITED RAMAN SPECTROSCOPY

With the advent of the laser, there was a rebirth of the Raman effect particularly with respect to polymers.[27] In theory, Raman spectroscopy should be a powerful probe of the polymer backbone as the nonpolar nature of the backbone results in weak IR absorption but strong Raman scattering.

Raman Spectroscopy of Elastomers

The early work in this area focused on elastomers and their unsaturated components[28–30] as the unsaturation was strongly Raman scattering and had high selectivity for the type of unsaturation. This exploratory work was followed by Raman investigations of the vulcanization of elastomers[31–34] as the polysulfidic linkages could be detected directly. Considerable insight into the mechanism of sulfur vulcanization was gained as a result.[35] However, no industrial sample could be studied as fluorescence interfered with the Raman spectra. Consequently, at this point in time, Raman spectroscopy had little analytical value for the rubber industry.

Raman Spectroscopy of Biopolymers in Aqueous Solutions

Due to the weak Raman scattering of water and the strong Raman scattering of the protein and nucleic acid backbones, Raman studies were particularly useful for determining the conformation of biopolymers in different environments.[36–40] It was possible to observe the helix-to-coil transitions in polypeptides[41] as well as the denaturation processes in proteins. Nucleic acids also ex-

hibit conformationally sensitive Raman spectra.[42,43] A general theory was developed to aid in the interpretation of spectral line shifts arising from conformational transitions.[44] Carbohydrates also exhibit Raman spectra which are sensitive to the substitution pattern and the crystalline phase.[45–47]

Normal Coordinate Analysis of Synthetic Polymers

With the development of Raman spectroscopy as a source of new vibrational information, it was necessary to enhance our band-assignment tools. As a result, normal coordinate analysis was developed.[48–52] Using normal coordinate analysis, it was possible to understand the structural basis of helix transitions and defects in polytetrafluoroethylene.[53] The band assignments for poly(vinyl fluoride) were made using normal coordinate analysis.[54] The limitation of the normal coordinate analysis, then and to this day, is the limited knowledge of the forces involved in the internal coordinates.[55] Substantial progress has been made, however, and it is likely that normal coordinate analysis will become a most powerful tool for structural analysis of vibrational spectra.

Raman Spectra of Surfaces and Interfaces

Because Raman spectroscopy is a scattering technique, it is intuitively obvious that the surface contribution should play an enhanced role in the observed Raman spectra. Utilizing this effect, it is possible to study the coupling agent, surfaces, and chemical reactions at interfaces using Raman spectroscopy.[56,57] One of the first applications of resonance Raman was the detection of a coupling agent on the surface of a glass fiber[58] which demonstrates the substantial enhancement of the signal due to resonance effects.

Because graphite fibers are black and highly absorbing, IR analysis is difficult but possible using special ATR techniques. On the other hand, Raman scattering has become the standard method of determining the nature of the crystallite size on the surface of graphite system.[59,60] The method is based on the observation of a Raman line for the ordered large crystals which is resolvable from a line due to the "disordered" small crystals of graphite.

FOURIER TRANSFORM INFRARED SPECTROSCOPY

The development of Fourier transform infrared spectroscopy (FTIR) revolutionized the use of IR for the study of polymers. First and foremost was the higher signal-to-noise ratios which yielded much improved spectra of polymers. Secondly, and especially important for applications of polymers, was the availability of digitized spectra which could be processed to remove baseline scattering and impurity absorbances, to normalize the spectra for differences in thicknesses, and to utilize chemometric procedures for quantitative analysis.[61] Signal-averaging techniques, which are possible with FTIR but quite difficult with dispersion instrumentation due to backlash effects, further improves the quality of the experimental spectra, making it possible to detect extremely small quantities of polymers including surface species.[62,63]

Absorbance Subtraction

The recognition of the utility of spectral subtraction to eliminate the intense interfering absorbances of the major components of the polymer spectra was important since the "difference" spectra could be magnified (absorbance scale-expanded) which improved the dynamic range of the measurements. The first example of absorbance subtraction was the application to the detection of structural defects in polychloroprene.[64,65] The spectra obtained are shown in Figure 1.

Examination of Figure 1 shows the spectra of *trans*-1,4-polychloroprene obtained at room temperature and at 80°C and the difference spectra. The difference spectra show the "crystalline" bands which are obtained by subtraction. The sharpness of the bands is indicative the high degree of local order which is expected for a crystalline phase. The utility of absorbance subtraction is to remove the interfering of the strong absorbing bands of polyethylene, revealing the degradation products developed by irradiation of polyethylene.[66] The mechanism of oxidation of *cis*-1,4-polybutadiene was revealed by utilizing spectral subtraction.[67] The small spectral effects produced by plasticization of poly(vinyl chloride) could be detected and characterized using spectral subtraction.[68]

Application of Least-Squares for Quantitative Analysis

With the availability of digitized spectra for all of the frequencies, the precision of the infrared measurement can be improved by utilizing all of the absorbances from all of the measured frequencies. The improvement in the signal-to-noise ratio of
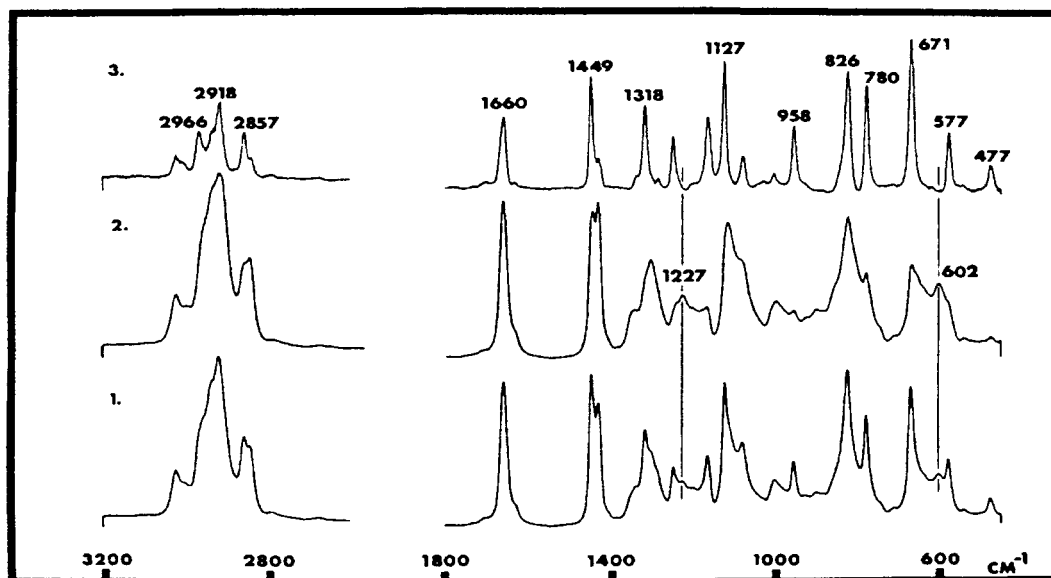
Figure 1 The spectrum of a cast film of predominately (>90%) *trans*-1,4-polychloroprene polymerized at −20°C (spectrum a) is compared with the same sample heated to −80°C (above the melting point) for 15 min (spectrum b). The "purified" crystalline isomer spectrum (spectrum c) exhibits the sharp band structure expected for a regular crystalline array. (See ref. 64).

the quantitative measurement is proportional to the square root of the number of frequencies. By applying least-squares refinement techniques, it is also possible to utilize spectra which have infrared bands that extensively overlap, which is always the case in the spectra of polymers.[69] The use of least-squares analysis was important for the study of the composition of epoxy systems,[70] the mechanism of crosslinking,[71] and the hydrolysis interaction with water.[72]

Chemometric Analysis of Multicomponent Polymer Systems

One of the basic problems in polymer quantitative analysis is the lack of suitable "standard" samples. For example, in studying conformations of polymers, it is difficult to have a model polymer which has a perfectly extended (e.g., *trans*) isomeric composition, and in similar fashion, a model polymer which has a perfectly bent (e.g., *gauche*) isomeric composition. One solution to this problem is to deconvolute the spectra of mixtures of different structural polymers into the contributions from the "pure" components. For two-component systems, this approach is termed the ratio method as it requires calculating the absorbance ratio of characteristic bands (bands which are characteristic of one of the structural compo-

nents) from mixture spectra in which the relative contributions of the two components are different.[73] This ratio technique was applied to the determination of the spectra of pure *trans* and *gauche* isomers of poly(ethylene terephthalate) (Fig. 2).[74]

SOLID-STATE NMR OF POLYMERS

Nuclear magnetic resonance (NMR) is one of the most important techniques for determining the microstructure of polymers.[76] Originally, the difficulty with analyzing polymer systems was the necessity of dissolving the polymers in a suitable solvent that did not interfere with the polymer resonances.[77] The dissolution process was time-consuming and often resulted in structural separations due to the insolubility of portions of the sample. The solution NMR results are highly specific and can measure structural differences between repeating units several units apart. In 1976, it was demonstrated that the NMR spectra of solids could be obtained using a series of special techniques including high-powered proton decoupling to remove the dipole–dipole interactions, magic angle spinning to minimize the chemical-shift anisotropy, and crosspolarization to increase the ^{13}C signal.[78] This development extended the
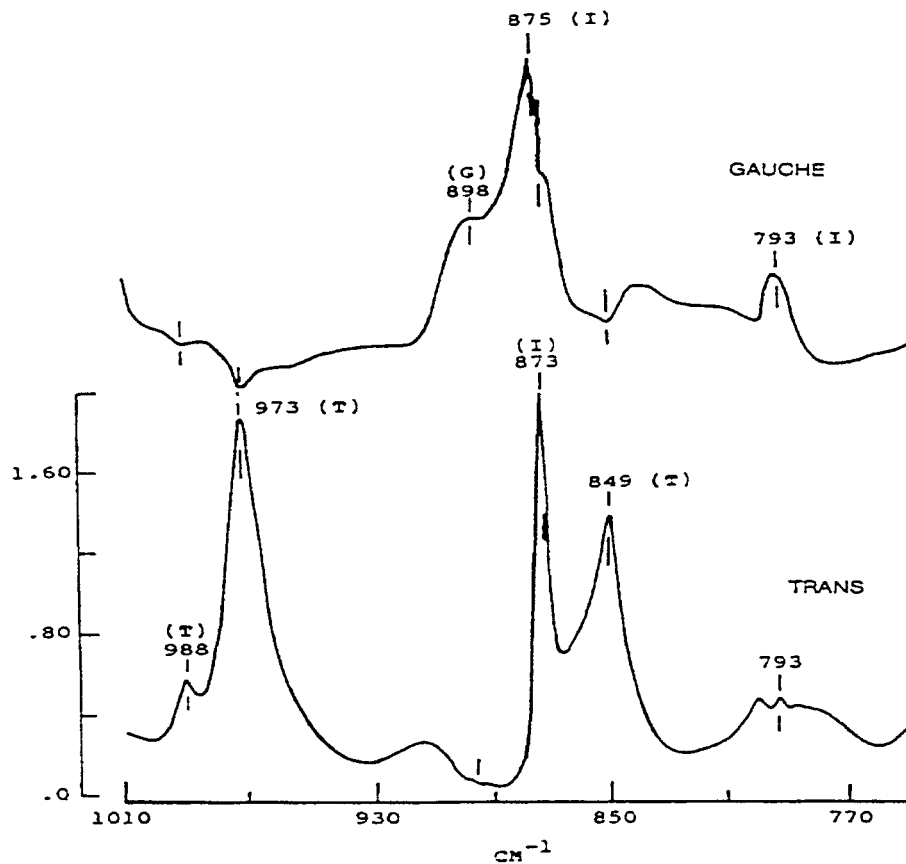
Figure 2 The computed pure spectra of the *trans* (T) and *gauche* (G) isomers of PET obtained by the ratio method. The letter I corresponds to an internal thickness band. (See ref. 75).

power and utility of NMR particularly as related not only to the chemical structure but also to the physical structure of the solid state.[79] Separation of resonances attributed to the amorphous and crystalline states of polymers was achieved.[80,81] The results for polyethylene are particularly useful as it is possible to follow the chemical reactions of the amorphous region.[82] The results are shown in Figure 3. This separation is accomplished by utilizing the differences in relaxation rates between the amorphous and crystalline phases in polyethylene.

Vulcanization of Elastomers

One of the advantages of solid-state NMR is the capability of studying insoluble systems such as networks[83,84] formed by polymerization and post-polymerization (vulcanization).[85] The sensitivity of the solid-state NMR technique to the chemical structure of vulcanized elastomers led to a series of studies which helped define the structure of a

number of different vulcanized elastomers.[86–100] In Figure 4, the solid-state NMR spectrum in the aliphatic region of the GHPD–MAS ^{13}C-NMR spectrum at 75.5 MHz of a high-*cis*-butadiene rubber vulcanizate cured with 10 phr of sulfur at 150°C for 30 min is shown. The result has been the development of considerably more insight into the mechanisms of vulcanization and methods of controlling the network structure.[101–103]

Structure of Polymer Blends

Many practical benefits can be obtained by blending polymers. Blending allows for the beneficial properties of two polymers to be combined in one material while shielding their mutual drawbacks. Deviations in the rule of mixing can lead to properties of the blend over and above those of its components. Thus, processability, chemical and environmental resistance, adhesion, and mechanical properties of polymer blends are superior to those of their homopolymers. However, most bi-
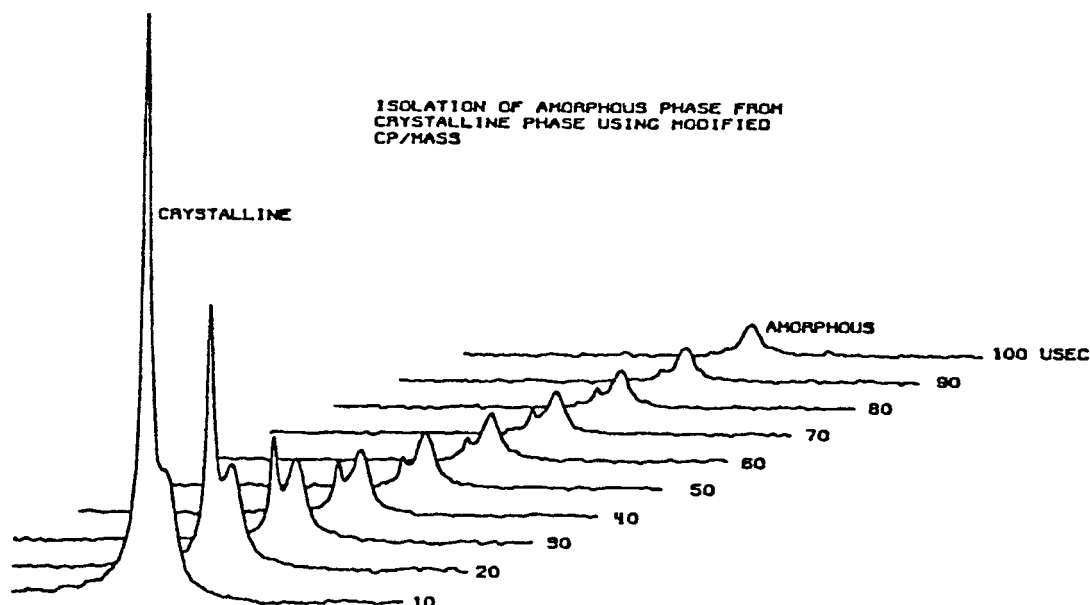
Figure 3 Stack plot of DD/CP/MAS spectra of HDPE. The delay times are indicated on the right side for each spectrum. The complete isolation of amorphous from the crystalline resonance is seen in the top spectrum (100 μs delay). (See ref. 82).

nary mixtures of polymers are not miscible on the molecular level because the entropy of mixing is not favorable for high molecular weight polymers. As most polymer pairs are immiscible, they form multiphase systems with weak physical and chemical interactions across the phase boundaries. As a result, immiscible blends exhibit poor mechanical properties. Miscible blends of two polymers can be engineered through specific interactions such as hydrogen bonding or van der Waals forces. Evidence for the specific intermolecular interactions that contribute to miscibility are most commonly obtained from optical clarity or T_g measurements using DSC, dielectric, or dynamical mechanical spectroscopy. IR[104] and NMR can be used to specifically identify the molecular-level interactions because the signals can be assigned to specific sites on the polymer chains. NMR has been used extensively to study the mixing of polymer blends and to characterize the specific intermolecular interactions.[105] Information about specific interactions can be obtained by measuring chemical-shift changes following blend formation[106] or by measuring dipolar couplings between pairs of protons or other nuclei on the polymer chains. The minimum requirement is that the resolution must be sufficiently high that separate signals can be resolved for the groups on the different polymer chains.[107]
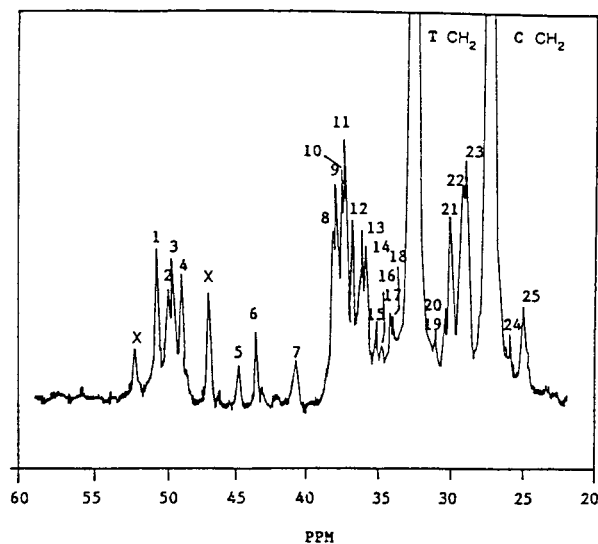
Figure 4 The aliphatic region of the GHPD–MAS 13C-NMR spectrum at 75.5 MHz of a high-*cis* butadiene rubber. Vulcanizate cure with 10 phr of sulfur at 150°C for 30 min. The x indicates a spinning sideband, and C CH_2 and T CH_2 are *cis* and *trans* CH_2, respectively. (See ref. 92).

Structure and Dynamics of Polymeric Liquid Crystals

Polymer liquid crystals (PLCs) are considered to be unique materials. PLCs are long-chain macro-

molecules which, due to a combination of inter-molecular orientation interactions and intrinsic stiffness, can orientationally order at low temperatures.[108]

The simplest view is that PLCs can be thought of as assemblies of liquid crystal molecules strung together by polymer strings or chains. This is certainly an oversimplification. Due to the antagonistic conflict between polymer backbone entropy (driving for disorder) and mesogenic orientational ordering (striving for order), the resultant PLC structure depends on the resolution of this antagonism. The distinctive features of these systems are due to the coupling between the nematic order and the configurations of the PLCs. As a result, the structures are unique and there are a number of mesomorphic properties which are unique to PLCs. The polymer chains are more than just strings and play a considerable role in the structure and molecular motions of the PLCs.

Solid-state NMR is a particularly powerful tool for the study of PLCs[109] as the chemical structure can be determined as well as the dynamics of the mesogen,[110] the spacer, and the polymer backbone.[111,112] The conformational changes that the PLC undergoes during a liquid crystalline transition can also be observed.[113] The molecular dynamics of polymer-dispersed liquid crystals have also been studied.[114,115]

NMR IMAGING

NMR is based on the fact that many atomic nuclei oscillate like tiny gyroscopes when in a magnetic field. In NMR, a sample is placed in a magnetic field which forces the nuclei into alignment. The sample is then bombarded with a radio wave. As the nuclei absorb the radio wave, they topple out of alignment with the magnetic field. As they lose the absorbed energy from the radio wave, they line up again. By measuring the specific radio frequencies that are emitted by the nuclei and the rate at which the realignment occurs, the spectroscopists can obtain detailed information about the molecular structure and motion of the sample they are studying.

Conventional NMR spectroscopy is used to determine chemical structure but cannot locate the position of the stimulated nuclei. NMR imaging (NMRI) is a method where the stimulating signal is spatially encoded so an image can be reconstructed showing the distribution of nuclei in the sample. Other than spatially encoding the signal, imaging works on the same principles as standard NMR.

The NMR imaging technique relies on the interaction of nuclei in only a small and controllable region of the sample by placing the sample in a spatially inhomogeneous magnetic field whose nuclear resonance frequency is matched to the RF signal in only that region. NMR imaging is involved in obtaining the spatial distribution of all parameters that NMR can detect. The NMR signals inherently depend on nuclear relaxation time constants T_1 and T_2, which, in turn, reflect the structural environment of the emitting nucleus. NMR is capable of providing information about molecular structure and motion; consequently, NMR imaging can provide a variety of structural factors measured *in situ*.

The spin densities and the molecular environments of the nuclei are reflected in the time variation of the amplitude of the measured rf signal and, hence, are reflected in the intensity of each voxel in the image. When the T_1's and T_2's are different in the voxels of a heterogeneous sample, these differences can be exploited to develop contrast in the NMR images. The pulse sequence that is usually used to measure the T_2 relaxation phenomena in images is called multiple spin–echo. At a given repetition time, TR, the NMR signal is measured at several different echo times, TE. These echoes provide a measure of the T_2 relaxation. By repeating the process at different TR values, the T_1 relaxation can also be measured.

Spatial resolution is limited by the smallest amount of sample that can be detected by NMR. Spatially resolving a given volume in an NMR image is equivalent to doing NMR spectroscopy on that volume. To resolve two spatially distinct volume elements requires the application of a magnetic-field gradient of sufficient strength such that the elements one wishes to resolve are shifted in resonance frequency from each other by an amount greater than the natural linewidth.

For a given magnetic field gradient strength, the spatial resolution in NMR imaging is determined by the line width:

$$\Delta x = \Delta \omega_{1/2}/G_x$$

where Δx is the spatial resolution, $\Delta \omega_{1/2}$ is the line width, and G_x is the gradient strength. For mobile liquids, the line widths are very narrow and high spatial resolution can be achieved. The attainable resolution is limited by spectroscopic

and hardware factors. Spectroscopic factors are the inherent line width and the spread of the chemical shift of an NMR signal, diffusion processes, and susceptibility gradients, both within the object and at its boundaries. Hardware factors may be the magnetic field inhomogeneity or instability, nonlinearity of the magnetic gradient field, and the achievable signal-to-noise ratio.

The difficulties of solid-state imaging arise since the solid-state line width is approximately 1000 times broader than its solution counterpart. Increasing the gradient by three or four orders of magnitude to maintain spatial resolution in solids imaging is a formidable task. Consequently, the normal NMRI experiment is the study of a mobile liquid probe in a polymer system.[116]

Diffusion in Polymers

Diffusion in polymers can be categorized into three general types: Fickian, anomalous, and Case II. Fickian diffusion describes the relationship of the mass flux of a penetrant to the concentration gradient present and can be characterized by an exponential decay in concentration with penetration into a material. The main feature of Case II diffusion is the constant concentration front throughout the imbibed region, while anomalous diffusion falls between the two extremes. Fickian diffusion often occurs in polymers which are at temperatures above their glass transition. This is because the polymer chains are in the rubbery state and possess sufficient mobility in which to allow solvent penetration. Fickian diffusion also commonly occurs when the activity of the solvent is sufficiently low and the diffusion therefore occurs only in the free volume of the polymer. Case II and anomalous diffusion are found primarily in polymers which are below their glass transition temperatures. At these lower temperatures, the polymer chains are not sufficiently mobile to immediately accommodate the solvent. Therefore, the polymer dynamics become important for the transport of small molecules through a matrix.

NMR imaging techniques have been used for the study of sorption and diffusion[117] as well as desorption[118,119] of multiple chemical substances[120] in polymeric materials. NMR imaging can directly provide the diffusion coefficients as a characteristic quantity of a liquid component in a sample, making it possible to map molecular migration on a microscopic scale. NMR imaging also provides additional information on the microdynamic and structural properties of heterogeneous

systems, such as subregion diameters, exchange times, and phase-boundary resistances.[121]

The principal advantage of NMR imaging is the possibility of making spatially localized diffusion measurements. One can examine by NMR imaging the concentration and location of a permeating liquid in a solid sample. A true diffusion parameter image is obtained where calculated diffusion coefficients are encoded into an intensity scale.

One of the obvious advantages of NMR imaging for the study of diffusion is the visual presentation of the data in the form of images. Such a presentation allows one to view directly the concentration and location of the penetrant and ignore extraneous factors influencing the diffusion.[122] Another advantage of NMR imaging is that it allows the study of samples of virtually any shape and allows the detection of initial imperfections in the sample being studied. It is generally difficult to interpret liquid-sorption measurements in solids because the samples being examined are not perfect, that is, they initially contain cracks and voids which increase both diffusion and uptake of the liquid. Also, the induced volumetric changes, although small, can cause microcracking or void formation.

Probing Spatially Inhomogeneous Polymer Systems

NMRI is particularly useful for the study of elastomer networks as the line widths of the proton resonances are narrow as the polymer is well above its glass transition. For elastomers, the proton NMR line widths are not excessively broad, T_2 is typically of the order of 10 ms, and imaging is possible with reasonably fast gradient switching (~ 250 μs or less), which can easily be achieved with most microimaging equipment. As a result of the narrow line width, the resolution of the images is high (down to a resolution of 20 μm). Additionally, the molecular sensitivity of the mobility enhances the contrast of the images. Consequently, NMRI has been useful in the determination of internal inhomogeneities[123] arising from inadequate mixing, gradients in crosslinking chemistry, filler distribution, and impurities.

The ordinary industrial accelerator systems generate a broad distribution of crosslink densities in rubber articles due to the poor mixing of the solid accelerator/sulfur recipe in the raw rubber. In particular, the variation in crosslink density leads to substantial differences in the coefficients of thermal expansion and high internal

stresses in the rubber article. These internal stresses limit the ultimate performance of the article whether in modulus or elongation.

Well-designed mixing protocols and carefully controlled cure cycles allow the development of a homogeneous distribution of the crosslinks in the final manufactured article. Mixing protocols can generate a well-dispersed accelerator system in the raw rubber. The NMR imaging technique can experimentally measure the homogeneity.

NMR imaging has been successful in studying the dispersion of crosslink density in traditional elastomers both along the chains as well as spatially (down to a resolution of 20 μm). These experimental observations have only recently been made and no opportunity has existed to develop these important new results into improved rubber products.

INFRARED IMAGING

Infrared microscopy for the analysis of small samples has made substantial progress with improvements in optics and the use of FTIR instrumentation. With the introduction of computer-controlled sample stages, it has been possible to perform infrared mapping using the computer stage to systematically reposition the sample. The mapping process can be automated. At the end of the experiment, the IR spectra can obtained from any of the spatially resolved pixels or a functional group map can be constructed by plotting the absorbances of the pixels in the map.

One of the obvious advantages of the microscope is the ability to focus on a portion of a small sample like a fiber. Fibers have always been difficult to obtain IR spectra as they have diameters that are optically thick from an IR point of view. With the microscope, one can use a rectangular aperture and focus on a portion of the fiber.[124,125] An extension of the microscopic field to mapping allows the study of the interphase in fiber-reinforced composites[126] and the permeation of moisture can be studied.[127]

The IR mapping of polymer-dispersed liquid crystals allows one to study the nature of the phase-separation process.[128,129] The details of the phase-separation process can be examined using the contact method of diffusion which involves placing the liquid crystal in contact with the polymer and following the phase separation after cooling[130] or polymerization.[131]

REFERENCES

1. J. L. Koenig and A. Van Roggen, *J. Appl. Polym. Sci.,* **9,** 359 (1965).
2. J. L. Koenig, *Spectrochim. Acta,* **22,** 1223 (1966).
3. J. L. Koenig, L. E. Wolfram, and J. Grasselli, *Spectrochim. Acta,* **20,** 1233 (1966).
4. J. L. Koenig, J. J. Mannion, and T. R. Evans, *J. Polym. Sci. A-2,* 401 (1966).
5. J. L. Koenig and D. E. Witenhafer, *Macromol. Chem.,* **99,** 193 (1966).
6. J. L. Koenig and M. J. Hannon, *J. Macromol. Sci., Phys. B,* **1,** 111 (1967).
7. D. E. Witenhafer and J. L. Koenig, *J. Macromol. Sci. Phys. B,* **2,** 235 (1968).
8. A. C. Angood and J. L. Koenig, *J. Appl. Phys.,* **39,** 4985 (1968).
9. J. L. Koenig and M. C. Agboatwalla, *J. Macromol. Sci. Phys. B,* **2,** 391 (1968).
10. P. D. Frayer, J. L. Koenig, and J. B. Lando, *J. Macromol. Sci. Phys. B,* **3,** 329 (1969).
11. J. L. Koenig and P. Vasko, *J. Macromol. Sci. Phys. B,* **4,** 369 (1970).
12. J. L. Koenig and P. Vasko, *J. Macromol. Sci. Phys. B,* **4,** 347 (1970).
13. W. O. Statton, J. L. Koenig, and M. Hannon, *J. Appl. Phys.,* **41,** 4290 (1970).
14. P. D. Vasko and J. L. Koenig, *J. Macromol. Sci. Phys. B,* **6,** 117 (1972).
15. P. D. Frayer, J. L. Koenig, and J. B. Lando, *J. Macromol. Sci. Phys. B,* **6,** 129 (1972).
16. J. L. Koenig and M. Itoga, *J. Macromol. Sci. Phys. B,* **6,** 309 (1972).
17. J. L. Koenig and M. Itoga, *J. Macromol. Sci. Phys. B,* **6,** 327 (1972).
18. J. L. Koenig, M. Ipekci, and J. B. Lando, *J. Macromol. Sci. Phys. B,* **6,** 713 (1972).
19. P. C. Painter, J. Havens, W. W. Hart, and J. L. Koenig, *J. Polym. Sci. Polym. Phys. Ed.,* **15,** 1223 (1977).
20. P. C. Painter, J. Havens, W. W. Hart, and J. L. Koenig, *J. Polym. Sci. Polym. Phys. Ed.,* **15,** 1237 (1977).
21. P. C. Painter, M. M. Coleman, and J. L. Koenig, *The Theory of Vibrational Spectroscopy and Its Application to Polymeric Materials,* Wiley-Interscience, New York, 1982.
22. J. L. Koenig and S. W. Cornell, *J. Polym. Sci. C,* 22 (1968).
23. J. L. Koenig, S. W. Cornell, and D. E. Witenhafer, *J. Polym. Sci. A2,* 301 (1967).
24. L. J. Fina and J. L. Koenig, *J. Polym. Sci. Polym. Phys.,* **24,** 2509 (1986).

25. L. J. Fina and J. L. Koenig, *J. Polym. Sci. Polym. Phys.,* **24,** 2525 (1986).
26. L. J. Fina and J. L. Koenig, *J. Polym. Sci. Polym. Phys.,* **24,** 2541 (1986).
27. J. L. Koenig, *Appl. Spectrosc. Rev.,* **4,** 233 (1971).
28. S. W. Cornell and J. L. Koenig, *J. Polym. Sci.,* **8,** 137 (1970).
29. S. W. Cornell and J. L. Koenig, *Rubber Chem. Tech.,* **43,** 313 (1970).
30. S. W. Cornell and J. L. Koenig, *Rubber Chem. Tech.,* **43,** 322 (1970).
31. R. S. Kapur, J. L. Koenig, and J. R. Shelton, *Rubber Chem.,* **47,** 911 (1974).
32. M. M. Coleman, J. L. Koenig, and J. R. Shelton, *J. Polym. Sci.,* **12,** 1001 (1974).
33. M. M. Coleman, J. R. Shelton, and J. L. Koenig, *Rubber Chem. Tech.,* **46,** 957 (1973).
34. M. M. Coleman, J. R. Shelton, and J. L. Koenig, *Rubber Chem. Tech.,* **46,** 938 (1973).
35. M. M. Coleman, J. R. Shelton, and J. L. Koenig, *Ind. Eng. Chem. Prod. Res. Dev.,* **13,** 154 (1974).
36. J. L. Koenig, *J. Polym. Sci. D,* **6,** 59 (1972).
37. J. L. Koenig and B. G. Frushour, *Biopolymers,* **11,** 2505 (1972).
38. B. G. Frushour and J. L. Koenig, *Biopolymers,* **14,** 649 (1975).
39. P. C. Painter and J. L. Koenig, in *Handbook of Biochemistry & Molecular Biology,* 3rd ed., G. D. Fasman, Ed., Plenum Press, New York, 1976, pp. 575–587.
40. B. G. Frushour and J. L. Koenig, *Biopolymers,* **14,** 649 (1975).
41. B. G. Frushour and J. L. Koenig, *Biopolymers,* **11,** 1871 (1972).
42. N. N. Aylward and J. L. Koenig, *Macromolecules,* **3,** 583 (1970).
43. N. N. Aylward and J. L. Koenig, *Macromolecules,* **3,** 590 (1970).
44. P. C. Painter and J. L. Koenig, *Biopolymers,* **15,** 241 (1976).
45. J. Blackwell, P. D. Vasko, and J. L. Koenig, *J. Appl. Phys.,* **41,** 4375 (1970).
46. P. D. Vasko, J. Blackwell, and J. L. Koenig, *Carbohydr. Res.,* **19,** 297 (1971).
47. B. G. Frushour and J. L. Koenig, *Biopolymers,* **14,** 379 (1975).
48. F. J. Boerio and J. L. Koenig, *J. Macromol. Sci. Rev. Macromol. Chem. C,* **7,** 209 (1972).
49. M. J. Hannon, F. J. Boerio, and J. L. Koenig, *J. Chem. Phys.,* **50,** 2829 (1969).
50. J. L. Koenig and F. J. Boerio, *J. Chem. Phys.,* **52,** 4170 (1970).
51. F. J. Boerio and J. L. Koenig, *J. Chem. Phys.,* **52,** 4826 (1970).
52. D. L. Tabb and J. L. Koenig, *J. Polym. Sci.,* **13,** 1159 (1975).
53. F. J. Boerio and J. L. Koenig, *J. Chem. Phys.,* **54,** 3667 (1971).
54. J. W. Hong, J. B. Lando, and J. L. Koenig, *Vibrat. Spectrosc.,* **3,** 55 (1992).
55. P. C. Painter and J. L. Koenig, *J. Polym. Sci. Polym. Phys. Ed.,* **15,** 1885 (1977).
56. C. H. Chiang, H. Ishida, and J. L. Koenig, *J. Coll. Int. Sci.,* **74,** 396 (1980).
57. C. H. Chiang and J. L. Koenig, *Polym. Comp.,* **1,** 88 (1980).
58. H. Ishida, J. L. Koenig, B. Asumoto, and M. E. Kenney, *Polym. Comp.,* **2,** 75 (1981).
59. F. Tuinstra and J. L. Koenig, *J. Compos. Mater.,* **4,** 492 (1970).
60. F. Tuinstra and J. L. Koenig, *J. Chem. Phys.,* **53,** 1126 (1970).
61. J. L. Koenig, *Appl. Spectrosc.,* **29,** 293 (1975).
62. H. Ishida and J. L. Koenig, *J. Coll. Int. Sci.,* **64,** 565 (1978).
63. S. R. Culler, H. Ishida, and J. L. Koenig, *Annu. Rev. Mater. Sci.,* **13,** 363 (1983).
64. M. M. Coleman, P. C. Painter, D. L. Tabb, and J. L. Koenig, *Polym. Lett.,* **12,** 577 (1974).
65. D. L. Tabb, J. L. Koenig, and M. M. Coleman, *J. Polym. Sci.,* **13,** 1145 (1975).
66. D. L. Tabb, J. J. Sevcik, and J. L. Koenig, *J. Polym. Sci.,* **13,** 815 (1975).
67. R. L. Pecsok, P. C. Painter, J. R. Shelton, and J. L. Koenig, *Rubber Chem. Tech.,* **49,** 1010 (1976).
68. D. L. Tabb and J. L. Koenig, *Macromolecules,* **8,** 929 (1975).
69. M. K. Antoon, J. H. Koenig, and J. L. Koenig, *Appl. Spectrosc.,* **31,** 518 (1977).
70. M. K. Antoon, B. E. Zehner, and J. L. Koenig, *Polym. Comp.,* **2,** 81 (1981).
71. M. K. Antoon and J. L. Koenig, *J. Polym. Sci. Polym. Chem. Ed.,* **19,** 549 (1981).
72. M. K. Antoon, J. L. Koenig, and T. Serefini, *J. Polym. Sci. Polym. Phys. Ed.,* **19,** 1567 (1981).
73. J. L. Koenig, L. D'Esposito, and M. K. Antoon, *Appl. Spectrosc.,* **31,** 292 (1977).
74. S. B. Lin and J. L. Koenig, *J. Polym. Sci. Polym. Phys. Ed.,* **21,** 2067 (1983).
75. S. B. Lin and J. L. Koenig, *J. Polym. Sci. Polym. Ed.,* **20,** 227 (1982).
76. J. L. Koenig, *Microstructure of Polymers,* Wiley, New York, 1982.
77. F. Bovey, *High Resolution Nuclear Magnetic Resonance of Macromolecules,* Academic Press, New York, 1972.
78. J. Schaefer and E. O. Stejskal, *J. Am. Chem. Soc.,* **98,** 1031 (1976).
79. C. A. Fyfe, *Solid State NMR for Chemists.* C. F. C. Press, Guelph, Canada, 1984.
80. A. L. Cholli, W. M. Ritchey, and J. L. Koenig, *Spectrosc. Lett.,* **16,** 21 (1983).
81. D. J. Patterson and J. L. Koenig, *Polymer,* **29,** 240 (1988).
82. A. L. Cholli, W. M. Ritchey, J. L. Koenig, and W. S. Veeman, *Spectrosc. Lett.,* **21,** 519 (1988).
83. E. Mertzel, D. Perchak, W. Ritchey, and J. L. Koenig, *Ind. Eng. Chem. Res.,* **27,** 580 (1988).
84. L. A. Weisenberger and J. L. Koenig, *J. Polym. Sci. Phys. Ed.,* **26,** 771 (1988).

85. D. J. Patterson and J. L. Koenig, *Appl. Spectrosc.,* **41,** 491 (1987).

86. J. L. Koenig and D. J. Patterson, *Elastom. Rubber Tech.,* **32,** 31 (1987).

87. A. M. Zaper and J. L. Koenig, *Rubber Chem. Tech.,* **60,** 252 (1987).

88. A. M. Zaper and J. L. Koenig, *Rubber Chem. Tech.,* **60,** 278 (1987).

89. M. Andreis and J. L. Koenig, *Polym. Prepr.,* **29,** 29 (1988).

90. A. M. Zaper and J. L. Koenig, *Makromol. Chem.,* **189,** 1239 (1988).

91. M. Andreis, J. Liu, and J. L. Koenig, *J. Polym. Sci. Polym. Phys. B,* **27,** 1389 (1989).

92. M. Andreis, J. Liu, and J. L. Koenig, *Rubber Chem. Tech.,* **62,** 82 (1989).

93. R. S. Clough and J. L. Koenig, *Rubber Chem. Tech.,* **62,** 908 (1989).

94. M. J. Krejsa and J. L. Koenig, *Rubber Chem. Tech.,* **64,** 40 (1991).

95. S. R. Smith and J. L. Koenig, *Rubber Chem. Tech.,* **65,** 176 (1992).

96. M. Krejsa and J. L. Koenig, *Rubber Chem. Tech.,* **65,** 427 (1992).

97. M. R. Krejsa and J. L. Koenig, *Rubber Chem. Tech.,* **66,** 73 (1993).

98. M. A. Rana and J. L. Koenig, *Rubber Chem. Tech.,* **66,** 242 (1993).

99. M. Mori and J. L. Koenig, *Rubber Chem. Tech.,* **68,** 551 (1995).

100. M. Mori and J. L. Koenig, *Rubber Chem. Tech.,* to appear.

101. M. R. Krejsa, J. L. Koenig, and A. B. Sullivan, *Rubber Chem. Tech.,* **67,** 348 (1994).

102. M. R. Krejsa and J. L. Koenig, *Rubber Chem. Tech.,* **66,** 376 (1993).

103. M. R. Krejsa and J. L. Koenig, in *Elastomer Technology Handbook,* N. P. Cheremisinoff, Ed., CRC Press, Boca Raton, FL, 1993, Chap. 11, pp. 475–491.

104. M. Sargent and J. L. Koenig, in *Structure Property Relations in Polymers, Advances in Chemistry Series 236,* M. W. Urban and C. D. Craver, Eds., American Chemical Society, Washington, DC, 1993, Chap. 6, pp. 191–219.

105. R. A. Grinsted and J. L. Koenig, *Polym. Prepr.,* **29,** 19 (1988).

106. R. A. Grinsted and J. L. Koenig, *J. Polym. Sci. Phys. Ed.,* **28,** 177 (1990).

107. R. A. Grinsted and J. L. Koenig, *Solid State NMR of Polymers,* L. J. Mathias, Ed., Plenum Press, New York, 1991, p. 131.

108. G. Sigaud, in *Phase Transitions in Liquid Crystals,* NATO ASI Series B: Physics, Vol. 290, S. Martellucci and A. N. Chester, Eds., Plenum Press, New York, 1992, p. 375.

109. R. L. Silvestri and J. L. Koenig, *Anal. Chim. Acta,* 997 (1993).

110. B. C. Perry and J. L. Koenig, in *Solid State NMR of Polymers,* L. J. Mathias, Ed., Plenum Press, New York, 1991, p. 215.

111. R. L. Silvestri, J. L. Koenig, W. R. Likavec, and W. M. Ritchey, *Polymer,* **36,** 2347 (1995).

112. R. L. Silvestri and J. L. Koenig, *Macromolecules,* **25,** 2341 (1992).

113. R. L. Silvestri and J. L. Koenig, *Polymer,* **35,** 2528 (1994).

114. K. L. Buchert, J. L. Koenig, and S. Q. Wang, *Appl. Spectrosc.,* **47,** 933 (1993).

115. K. L. Buchert, J. L. Koenig, and S. Q. Wang, *Appl. Spectrosc.,* **47,** 942 (1993).

116. J. L. Koenig, *Spectroscopy of Polymers, American Chemical Society,* Washington, DC, 1992.

117. L. A. Weisenberger and J. L. Koenig, *Macromolecules,* **23,** 2445 (1990).

118. L. A. Weisenberger and J. L. Koenig, *Macromolecules,* **23,** 2454 (1990).

119. R. A. Grinsted, L. Clark, and J. L. Koenig, *Macromolecules,* **25,** 1235 (1992).

120. R. A. Grinsted and J. L. Koenig, *Macromolecules,* **25,** 1229 (1992).

121. J. L. Koenig, in *Characterization of Composite Materials,* H. Ishida and L. E. Fitzpatrick, Eds., Butterworth–Heinemann, 1994, Chap. 3, pp. 44–62.

122. E. Shaw, W. R. Williams, and J. L. Koenig, *Ophthal. Res.,* **27,** 268 (1995).

123. R. S. Clough and J. L. Koenig, *J. Polym. Sci. Lett.,* **27,** 451 (1989).

124. A. Mavrich, F. Fondeur, H. Ishida, H. D. Wagner, and J. L. Koenig, *J. Adhes.,* **46,** 91 (1994).

125. A. M. Mavrich, H. Ishida, and J. L. Koenig, *Appl. Spectrosc.,* **49,** 149 (1995).

126. C. D. Arvanitopoulos and J. L. Koenig, *Appl. Spectrosc.,* **50,** 1 (1996).

127. C. D. Arvanitopoulos and J. L. Koenig, *Appl. Spectrosc.,* **50,** 11 (1996).

128. S. R. Challa, S. Q. Wang, and J. L. Koenig, *Appl. Spectrosc.,* **49,** 267 (1995).

129. C. A. McFarland, J. L. Koenig, and J. L. West, *Appl. Spectrosc.,* **47,** 598 (1993).

130. S. R. Challa, S. Q. Wang, and J. L. Koenig, *Appl. Spectrosc.,* **50,** 1339 (1996).

131. S. R. Challa, S.-Q. Wang, and J. L. Koenig, *Appl. Spectrosc.,* to appear.